

## A STOCHASTIC-SPECTRAL FINITE ELEMENT METHOD FOR ANALYSIS OF ELASTO-DYNAMIC PROBLEMS

Pooya ZAKIAN

*Ph.D. student of Earthquake Engineering, Faculty of Civil and Environmental Engineering,  
Tarbiat Modares University, P.O. Box 14115-397, Tehran, Iran  
p.zakian@modares.ac.ir*

Naser KHAJI

*Professor of Earthquake Engineering, Faculty of Civil and Environmental Engineering,  
Tarbiat Modares University, P.O. Box 14115-397, Tehran, Iran  
nkhaji@modares.ac.ir*

**Keywords:** Stochastic Finite Element Method, Spectral Finite Element Method, Karhunen–Loève Expansion, Polynomial Chaos expansion, Stochastic seismic Analysis

### ABSTRACT

A stochastic-spectral finite element method is presented and applied to elastodynamic problems in this research paper. The presented method is a new hybridized numerical method incorporating stochastic finite element and spectral finite element methods. Although spectral finite element is a well-established method for solving elastodynamic problems such as wave propagation, it cannot consider randomness in its standard form. On the other hand, analysis of stochastic engineering systems is undergoing a revolution considering the advances in computers. Therefore, this research proposes a spectral finite element method reformulated by stochastic finite element method to solve linearly stochastic elastodynamic problems. Diagonal mass matrix, accelerated pre-processing stage (Karhunen–Loève expansion) and reduction of mesh number maintaining suitable accuracy are the main advantageous of the proposed method which apart from new abilities, uses the features of the both methods in order to solve stochastically linear elastodynamic problems with suitable computational efficiency and accuracy. Two numerical examples are prepared to demonstrate advantages of the proposed stochastic spectral finite element method.

### INTRODUCTION

Stochastic methods can be applied to many fields including structural mechanics, solid mechanics, fluid mechanics, fluid-structure interaction, soil-structure interaction and so forth. These methods are usually deals with uncertainty quantification and reliability assessment of systems due to randomness of material properties, geometry, loading, and so on. Stochastic finite element method (StFEM) is one of the favorite numerical methods for analysis of engineering systems with uncertain properties. StFEM is a developed version of deterministic FEM for considering the random fluctuation of structural properties, and loadings such as earthquake, wind, and wave loads. There are many studies focused on the StFEM, among which, a few of them are concisely discussed here. Stochastic finite element analysis of elastostatic problems with perturbation based approach was carried out by (Kamishi, 2008). A simulation program for probabilistic structural analysis was developed by (Shang and Yun, 2013).

Spectral finite element method (SFEM) is a numerical method originally proposed for wave propagation problems to utilize its high accuracy and excellent convergence properties. The SFEM is fundamentally a combination of two different methods of spectral element method and the FEM. The SFEM was firstly presented by (Patera, 1984) in computational fluid dynamics and was then applied to various types of wave propagation problems. Solution of elastostatic and elastodynamic problems using Chebyshev

SFEM was performed by (Dauksher and Emery, 2000). Time domain spectral finite element analysis of transient elastodynamic problems was accomplished by (Khaji et al., 2009). Analysis of two-dimensional (2D) elastostatic and wave propagation problems employing several examples in order to demonstrate capability of spectral finite element method was performed by (Witkowski, Rucka et al., 2012). Also, application of spectral finite element to seismic wave propagation was fulfilled by (Komatitsch et al., 2002). In this paper, a combination of stochastic finite element and spectral finite element methods as a numerical technique for uncertainty quantification is proposed. This study uses an improved version of the StFEM for the combination which is called StFEM with spectral decomposition, established by (Ghanem and Spanos, 2003). On the other hand, SFEM has the strategy of employing special orthogonal polynomials (e.g., Lobatto) and quadrature schemes (e.g., Gauss-Lobatto-Legendre), leading to suitable accuracy, and much less domain discretization with excellent convergence as well. The proposed method, which is called StSFEM, simultaneously comprises the advantages of both methods for solving stochastically linear elastodynamic problems with appropriate computational efficiency and accuracy. Moreover, spectral finite element is also proposed for numerical approximation of Fredholm integral equation followed by the proposed method to enhance the efficiency of this method.

## STOCHASTIC SPECTRAL FINITE ELEMENT METHOD (StSFEM)

### Basic definitions of StSFEM

In this section, a numerical technique that is called stochastic spectral finite element method (StSFEM) is presented. This new method transforms the deterministic SFEM to stochastic SFEM. For this purpose, three essential points should be concerned in implementation of spectral finite elements to stochastic condition: (a) interpolation functions, (b) numerical integration, and (c) computational efficiency. Here, a general 2D form of stochastic spectral finite element is presented.

Assume a complete probability space  $(\Omega, \mathfrak{F}, P)$  with sample space  $\Omega$ ,  $\mathfrak{F}$ -algebra on  $\Omega$  and probability measure  $P$  on  $\mathfrak{F}$ . A real random field  $w$  defined on a set  $D$  is a mapping  $w: D \times \Omega \rightarrow \mathfrak{R}$  such that, for each  $\mathbf{x} \in D$ ,  $w(\mathbf{x}, \cdot)$  implies a random variable with respect to  $(\Omega, \mathfrak{F}, P)$ . The random field  $w$  at the point  $\mathbf{x} \in D$  is a random variable, while a real number  $w(\mathbf{x}, \omega)$  for each realization  $\omega \in \Omega$  is obtained.  $w(\mathbf{x}, \cdot)$  is also considered as a sample drawn from an appropriate function space so that each realization  $\omega$  gives a function on  $D$ . Mathematical background and basic definitions of probability space and measure theory are being referred to (Bobrowski, 2005).

Any random field  $w: D \times \Omega \rightarrow \mathfrak{R}$  with a continuous covariance function may be represented as a KLE given by

$$w(\mathbf{x}, \xi) = w(\mathbf{x}) + \sum_{i=1}^{\infty} \sqrt{\lambda_i} w_i(x) \zeta_i(\omega) \quad (1)$$

where this series converges in the Hilbert space. Furthermore,  $\{\zeta_i\}_{i=1}^{\infty}$  represents a sequence of uncorrelated random variables in  $L^2_p(\Omega)$  with zero mean and unit variance. The aforementioned random field could be Young's modulus of a structure, for example. As a special case, the interpolation function matrix of a spectral element with  $n_l = 3$  is defined as

$$\mathbf{H} = \begin{bmatrix} N_1 & 0 & N_2 & 0 & N_3 & 0 & \cdots & N_{14} & 0 & N_{15} & 0 & N_{16} & 0 \\ 0 & N_1 & 0 & N_2 & 0 & N_3 & \cdots & 0 & N_{14} & 0 & N_{15} & 0 & N_{16} \end{bmatrix} \quad (2)$$

Based on the principal of virtual work, displacement-based stochastic finite element solution can be derived as

$$\int_V \bar{\mathbf{u}}^T \mathbf{f}_B dV + \int_{S_f} \bar{\mathbf{u}}_{s_f}^T \mathbf{f}_{s_f} dS + \sum_i \bar{\mathbf{u}}_i^T \mathbf{R}_C^i \quad (3)$$

in which  $\bar{\mathbf{u}}$  and  $\bar{\boldsymbol{\epsilon}}$  denote virtual displacement and the corresponding virtual strain, respectively.  $\mathbf{f}_B$ ,  $\mathbf{f}_{s_f}$  and  $\mathbf{R}_C^i$  are body force, surface force and nodal concentrated load vectors, respectively. After expanding and multiplying by  $\bar{\mathbf{U}}^T$ , one may have



$$\begin{aligned} \bar{\mathbf{U}}^T \sum_e \int_{V^{(e)}} \mathbf{u}^{(e)T} \mathbf{f}_b^{(e)} dV^{(e)} &= \bar{\mathbf{U}}^T \sum_e \int_{V^{(e)}} \bar{\mathbf{u}}^{(e)T} \mathbf{f}_b^{(e)} dV^{(e)} + \bar{\mathbf{U}}^T \sum_e \int_{S_f^{(e)}} \bar{\mathbf{u}}_{s_f}^{(e)T} \mathbf{f}_{s_f}^{(e)} dS^{(e)} + \\ \bar{\mathbf{U}}^T \sum_i \bar{\mathbf{u}}_i^T \mathbf{R}_c^i & \end{aligned} \quad (4)$$

Using the following interpolation functions and strain-displacement relationships in stochastic form

$$\mathbf{u}^{(e)} = \mathbf{C}^{(e)} \bar{\mathbf{U}}^{(e)}, \quad \boldsymbol{\varepsilon}^{(e)}(x, y, z, t) = \mathbf{B} \bar{\mathbf{U}}^{(e)}(x, y, z, t), \quad \bar{\mathbf{u}}^{(e)}(x, y, z, t) = \mathbf{H} \bar{\mathbf{U}}^{(e)}(x, y, z, t) \quad (5)$$

If inertia and damping forces are being supposed as a contribution in body force, the following form may be easily derived

$$\begin{aligned} \bar{\mathbf{U}}^T \sum_e \int_{V^{(e)}} \mathbf{B}^{(e)T} \mathbf{C}^{(e)} \mathbf{B}^{(e)} dV^{(e)} \ddot{\mathbf{U}} - \bar{\mathbf{U}}^T \sum_e \int_{V^{(e)}} \mathbf{H}^{(e)T} [\mathbf{f}_b^{(e)} - \dots \mathbf{H}^{(e)} \ddot{\mathbf{U}} - \mathbf{C}^{(e)} \dot{\mathbf{U}}] dV^{(e)} & \\ + \bar{\mathbf{U}}^T \sum_e \int_{S_f^{(e)}} \mathbf{H}^{s(e)T} \mathbf{f}_{s_f}^{(e)} dS^{(e)} + \bar{\mathbf{U}}^T \mathbf{R}_c & \end{aligned} \quad (6)$$

After some mathematical manipulations, and imposing truncated KLE and PCE, the following expression may be derived

$$\mathbf{M} \sum_{j=0}^P \ddot{\mathbf{U}}_j(t) \Psi_j(\mathbf{u}) + \mathbf{C} \sum_{j=0}^P \dot{\mathbf{U}}_j(t) \Psi_j(\mathbf{u}) + \left( \sum_{i=0}^M \mathbf{K}_{i < i}(\mathbf{u}) \right) \sum_{j=0}^P \mathbf{U}_j(t) \Psi_j(\mathbf{u}) = \mathbf{R}_b(t) + \mathbf{R}_s(t) + \mathbf{R}_c(t) \quad (7)$$

in which  $\mathbf{M}$ ,  $\mathbf{C}$  and  $\mathbf{K}$  indicates mass, damping and stiffness matrices, respectively. In addition,  $\mathbf{R}_b(t)$ ,  $\mathbf{R}_s(t)$ , and  $\mathbf{R}_c(t)$  denote body force, surface force and concentrated force vectors, respectively. In order to achieve the optimal approximation of the exact solution  $\mathbf{U}(\mathbf{u})$  in the space spanned by the PCE, the residual obtained from the both side of Eq. (7) multiplied by  $\Psi_k(\mathbf{u})$  should have a mathematical expectation of zero. Thus, multiplying the both sides of Eq. (7) by  $\Psi_k(\mathbf{u})$ , and taking mathematical expectation leads to

$$\begin{aligned} \langle \Psi_k(\mathbf{u}) \mathbf{M} \sum_{j=0}^P \ddot{\mathbf{U}}_j(t) \Psi_j(\mathbf{u}) \rangle + \langle \Psi_k(\mathbf{u}) \mathbf{C} \sum_{j=0}^P \dot{\mathbf{U}}_j(t) \Psi_j(\mathbf{u}) \rangle + \\ \langle \Psi_k(\mathbf{u}) \left( \sum_{i=0}^M \mathbf{K}_{i < i}(\mathbf{u}) \right) \sum_{j=0}^P \mathbf{U}_j(t) \Psi_j(\mathbf{u}) \rangle = \langle \Psi_k(\mathbf{u}) \mathbf{R}_b(t) \rangle + \langle \Psi_k(\mathbf{u}) \mathbf{R}_s(t) \rangle + \langle \Psi_k(\mathbf{u}) \mathbf{R}_c(t) \rangle \end{aligned} \quad (8)$$

Therefore, dynamic equilibrium of stochastic finite element analysis is summarized as

$$\mathbf{M}_{st} \ddot{\mathbf{U}}(\mathbf{u}) + \mathbf{C}_{st} \dot{\mathbf{U}}(\mathbf{u}) + \mathbf{K}_{st} \mathbf{U}(\mathbf{u}) = \mathbf{F}_{st} \quad (9)$$

Obviously,  $\mathbf{R}$  and  $\mathbf{U}$  vectors are functions of time in a dynamic equilibrium. As already mentioned,  $\mathbf{M}$  is a diagonal matrix based upon the SFEM, and hence  $\mathbf{M}_{st}$  will be diagonal, too. This statement may be readily proved due to the fact that  $\langle \Psi_k^2(\mathbf{u}) \rangle \mathbf{M}$  is a block-diagonal matrix, in which each block matrix is in a diagonal form.

The Rayleigh relationship can be used for the damping matrix  $\mathbf{C}$ . However, the damping matrix may be generated with deterministic mass and mean stiffness matrices in the Rayleigh technique, to neglect the randomness of the damping matrix due to the stochastic stiffness matrix. Evaluation of response statistics from the solution vector, including mean response value and response variance, is obtained by the following forms

$$\begin{aligned} \langle \mathbf{u} \rangle &= \mathbf{c}_0 \\ \text{cov}[\mathbf{u}, \mathbf{u}] &= \sum_{j=1}^P \langle \Psi_j^2 \rangle \mathbf{c}_j \mathbf{c}_j^T \end{aligned} \quad (10)$$

where  $\langle \mathbf{u} \rangle$  is mean value of the response, and  $\text{cov}[\mathbf{u}, \mathbf{u}]$  denotes variance of the response. In the case of dynamic analysis, Eq. (10) is utilized at each time instance for post-processing stage.

*Numerical eigenvalue analysis of Fredholm equation with the SFEM*

There are many investigations on the solution of Fredholm integral equation, among which the FEM and wavelet based methods which can be found in (Ghanem and Spanos, 2003, Ziari et al., 2012). Here, the SFEM is proposed for this numerical solution, and is then inserted into the proposed StSFEM to solve the eigenvalue problem of Fredholm integral equation associated with the KLE as

$$\int_{-a}^a \int_{-a}^a C(x_1, y_1; x_2, y_2) w_n(x_2, y_2) dx_2 dy_2 = \lambda_n w_n(x_1, y_1) \quad (11)$$

The procedure of spectral element approximation of the problem implies subdividing the domain into  $N_s$  spectral elements leading to the following discrete form of eigenvalue analysis

$$\mathbf{C}\mathbf{D} = \mathbf{B}\mathbf{D} \quad (12)$$

in which the  $j$ th column of  $\mathbf{D}$  matrix is the nodal value corresponding to the  $j$ th eigenfunction including the relevant  $\mathbf{d}$  vector, while diagonal terms of matrix consist of eigenvalues.  $\mathbf{C}$  and  $\mathbf{D}$  are calculated by assembling of the following matrix representations

$$\mathbf{C}_{e_1 e_2} = \int_{A^{e_1}} \int_{A^{e_2}} C(x_1, y_1; x_2, y_2) \mathbf{H}^{e_1 T}(r_1, s_1) \mathbf{H}^{e_2}(r_2, s_2) dA^{e_1} dA^{e_2} \quad (13)$$

and

$$\mathbf{B}_{e_1 e_2} = \int_{A^{e_1}} \mathbf{H}^{e_1 T}(r, s) \mathbf{H}^{e_2}(r, s) dA^{e_1} \quad (14)$$

where  $\mathbf{B}_{e_1 e_2}$  is similar to construction of a mass matrix with unit mass density in the SFEM procedure. Since the SFEM produces diagonal mass matrices due to Lobatto polynomial and the GLL quadrature, therefore  $\mathbf{B}_{e_1 e_2}$  is a so-called *mass-like* matrix that is in diagonal form. This diagonal matrix reduces the complexity of the eigenvalue problem having great computational efforts. As an alternative approach, one may easily inverse the  $\mathbf{B}$  matrix, and convert the non-standard eigenvalue problem of Eq. (12) to the standard form. A few discretizations are also required with respect to the FEM discretization. In the SFEM, since the numerical GLL integration points are placed exactly on the nodes of the element, one may only use the  $\mathbf{D}$  matrix in order to solve the Eq. (12). Accordingly, it is not necessary to make the eigenfunction polynomial using the following equation

$$w_n(x, y) \cong \sum_{e=1}^N \mathbf{H}^e \mathbf{d}_n^e \quad (15)$$

which takes significant computational efforts. This point reveals another privilege of the present method.

## ILLUSTRATIVE EXAMPLES

In this part, two numerical examples are solved to verify the proposed StSFEM. These examples are solved with three methods of the Monte-Carlo Simulation (MCS), the StSFEM, and the proposed StSFEM. In the case of the MCS, the number of simulations is selected as 10,000. Furthermore, the KLE is employed for considering the covariance function. Random parameters utilized in the examples are assumed to be



Gaussian with exponential covariance function. The Newmark- $\beta$  (average acceleration) is employed for temporal discretization.

#### A random clamped plate subjected to seismic loading

Stochastic seismic analysis of a clamped square plate of unit dimensions (Fig. 1) subjected to El-Centro earthquake record (Fig. 2) is examined as the first example, in which Young's modulus is a random parameter. Fig. 1 also depicts the mesh densities of the StFEM and the StSFEM, in which 64 finite elements are employed for the MCS and the StFEM, while only 4 spectral finite elements are utilized for the StSFEM.

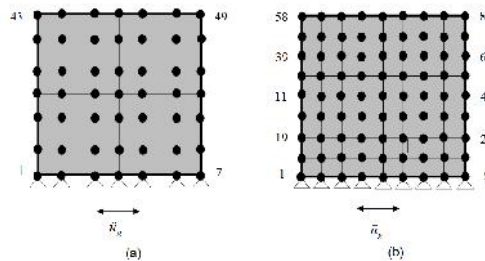


Figure 1. A clamped plate with random modulus of elasticity subjected to seismic load: (a) the StFEM and (b) the StSFEM meshes.

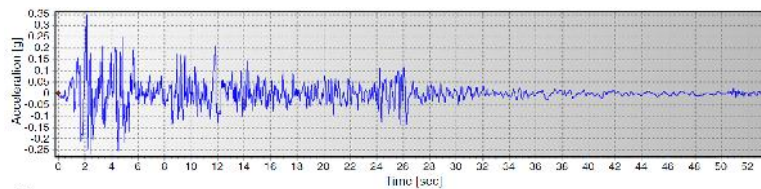


Figure 2. El-Centro (N-S component, 1940) earthquake record.

In this example, 2D plane stress condition is assumed. Dynamic analysis of the clamped plate is performed using time interval of 0.02 sec., and the damping ratio of the plate is considered as 5 per cent. The governing equation of this problem (Eq. (9)) can be rewritten as

$$\mathbf{M}\ddot{\mathbf{U}}(t) + \mathbf{C}\dot{\mathbf{U}}(t) + \mathbf{K}_{st}\mathbf{U}(t) = -\mathbf{M}\mathbf{r}\ddot{u}_g \quad (16)$$

in which  $\mathbf{r}$  denotes an influence vector implying the direction of excitation, and  $\ddot{u}_g$  is the ground acceleration. All relevant parameters of the problem are mentioned in Table 1.

Table 1. Parameters considered for the clamped plate

Variable	Value
Mass density	0.5 kg/m <sup>3</sup>
Mean value of Young's modulus	1.0 N/m <sup>2</sup>
Standard deviation of Young's modulus	0.2 N/m <sup>2</sup>
Poisson's ratio	0.2
Correlation length in x direction	1 m
Correlation length in y direction	1 m

The response histories of the StFEM and StSFEM are plotted and compared in Fig. 3, in which negligible differences are observed between the responses of two methods. In addition, Table 2 provides the extremum values of displacement responses at the edge node of clamped plate. Although only four elements are used for the StSFEM, it indicates desirable accuracy in comparison with the StFEM. As mentioned before, mass matrix becomes diagonal in the StSFEM procedure, which leads to remarkable computational advantage.

Table 2. Maxima and minima of displacement response histories at the edge node of the clamped plate obtained by various methods

Parameters	Stochastic analysis method		
	MCS	StFEM	StSFEM
Maximum mean values	13.7668	13.9650	14.4761
Maximum standard deviations	3.6904	3.7249	3.8058
Minimum mean values	-12.8463	-13.2259	-12.9134
Minimum standard deviations	0	0	0

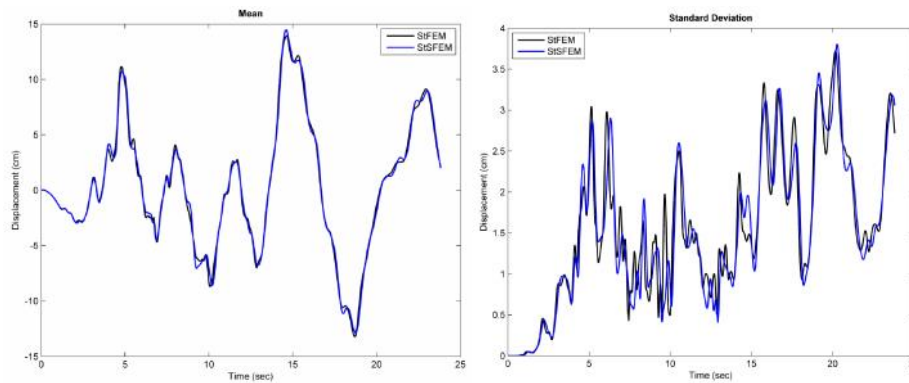


Figure 3. Comparison of response histories of the clamped plate obtained by the StFEM and the StSFEM: (a) mean values, and (b) standard deviations

#### Random Cook's structure subjected to dynamic loading

Here, the well-known plane stress Cook's membrane structure is analyzed as a structure with random Young's modulus subjected to Heaviside dynamic load as illustrated in Fig. 4.

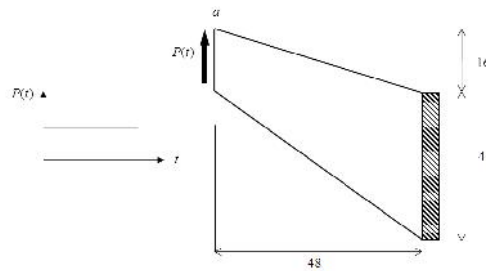


Figure 4. Geometry and load properties of the Cook's structure.

This problem is selected as an example requiring a distorted mesh. Thus, it is useful for assessment of the StSFEM's efficiency and accuracy. In this example, Eq. (9) is modified as

$$\mathbf{M}\ddot{\mathbf{U}}(\mathbf{r}) + \mathbf{K}_{st}\mathbf{U}(\mathbf{r}) = \mathbf{P} \quad (17)$$

Table 3 indicates the parameters of this example. As the StFEM usually uses the FEM for numerical solution of Fredholm integral equation, the StSFEM is thus adjusted to use the SFEM for this solution, as already explained. The MCS and the StFEM utilize a  $13 \times 10$  mesh, whereas the proposed StSFEM uses a  $4 \times 3$  mesh in both stages of the solution of Fredholm equation and stochastic analysis. The first six largest modes are incorporated for the stochastic analysis, and hence stochastic stiffness matrix becomes 84-fold of its deterministic counterpart. Comparison of six eigenvalues determined by the FEM and the SFEM are listed in Table 4, demonstrating the accuracy of the SFEM compared to the FEM in numerical solution of Fredholm integral equation. Fig. 5 shows deformation mean values and standard deviations of the structure at the end of analysis (i.e.,  $t = 10$  sec.) with time interval of 0.005 sec. Response time histories at node  $a$  analyzed by the StFEM and the StSFEM are also compared in Fig. 6. Considering the number of elements utilized for each method, the StSFEM provides suitable accuracy and computational efficiency. In addition to the computational efficiency in the stochastic analysis, it should be noted that this efficiency is also appeared in Fredholm integral solution. In the cases of the MCS and the StFEM, mass matrices are block-diagonal rather than diagonal, while the mass matrix produced by the StSFEM is diagonal. Although identical numbers of DOFs are being considered for both StFEM and StSFEM, analysis of the StFEM is much more time-consuming than the StSFEM analysis. Despite only twelve elements are employed in the StSFEM, it shows desirable accuracy compared to the StFEM's outcomes. Also, Table 5 illustrates the extremum values of displacement responses for better evaluation.

**Table 3. Parameters considered for the Cook's structure with all consistent parameters**

Variable	Value
Mass density	0.0001
Mean value of Young's modulus	1.0
Standard deviation of Young's modulus	0.1
Poisson's ratio	1/3
Correlation length in $x$ direction	48
Correlation length in $y$ direction	60

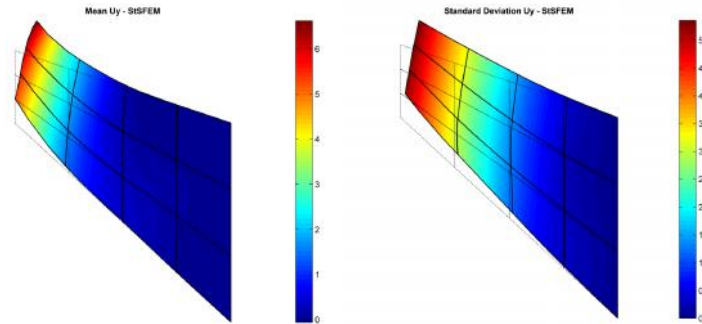


Figure 5. Vertical displacement field of the Cook's structure at the end of dynamic analysis obtained by the StSFEM: mean values and standard deviations

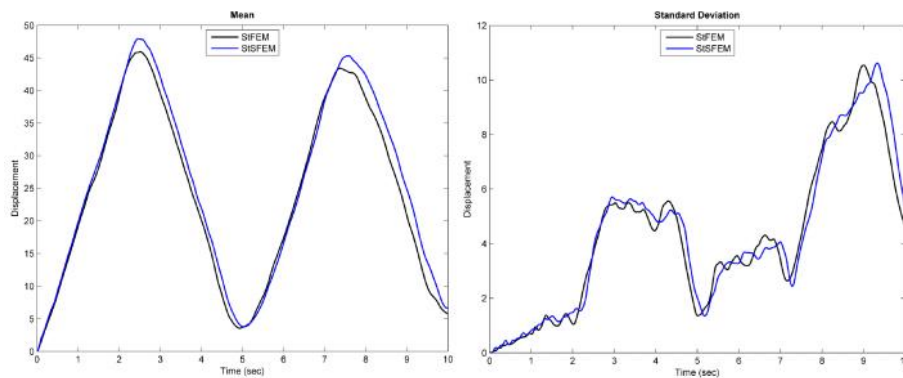


Figure 6. Comparison of vertical displacement response histories of the Cook's structure tip node a computed by the StFEM and the StSFEM: mean values and standard deviations

**Table 4. Eigenvalues' comparisons of the KLE using numerical eigensolution of Fredholm integral equation for the Cook's structure**

Mode number	Eigensolution method	
	FEM	SFEM
1	8.75350962	8.77398726
2	2.02222342	2.04019824
3	0.66839825	0.68262309
4	0.58926372	0.59891365
5	0.31772350	0.32862539
6	0.28178652	0.29592506

**Table 5. Maxima of displacement response histories at the tip node of Cook's structure obtained by various methods**

Parameters	Stochastic analysis method		
	MCS	StFEM	StSFEM
Maximum mean values	45.9289	45.9330	47.9483
Maximum standard deviations	10.1110	10.5418	10.6178

## CONCLUSIONS

In this paper, stochastic dynamic analyses are carried out by the presented StSFEM. This method contains some remarkable features such as diagonal mass matrix, and reduced domain discretization, leading to favorable computational accuracy and effort. Additionally, the SFEM is employed to solve Fredholm integral equation during the StSFEM procedure. This suggestion makes the proposed StSFEM more efficient. These efficiencies are mentioned as follows: (1) the *mass-like* matrix in eigensolution of Fredholm integral equation becomes diagonal, and hence one can easily transform the non-standard eigenvalue problem to standard form; (2) larger mesh size can be selected respect to the FEM discretization which requires smaller mesh size; (3) since the discrete nodal values obtained from the SFEM numerical solution are directly applicable into the quadrature, it is not necessary to construct eigenfunctions with the interpolation functions. The efficiency and accuracy of the proposed method have been demonstrated by the numerical examples. The StSFEM can also be extended to seismic wave propagation problem which is in progressive state of study by the authors.

## REFERENCES

- Bobrowski A (2005) Functional Analysis for Probability and Stochastic Processes: An Introduction, Cambridge University Press
- Dauksher W and Emery AF (2000) The solution of elastostatic and elastodynamic problems with Chebyshev spectral finite elements, *Computer Methods in Applied Mechanics and Engineering*, **188**(1–3): 217-233
- Ghanem R G and Spanos PD (2003) Stochastic Finite Elements: A Spectral Approach, Courier Dover Publications.
- Kami ski, M. (2008) On stochastic finite element method for linear elastostatics by the Taylor expansion, *Structural and Multidisciplinary Optimization*, **35**(3): 213-223
- Khaji N, Habibi M and Mirhashemian P (2009) Modeling transient elastodynamic problems using spectral element method, *Asian Journal of Civil Engineering (Building and Housing)*, **10**(4): 361-380
- Komatitsch D, Ritsema J and Tromp J (2002) The Spectral-Element Method, Beowulf Computing, and Global Seismology, *Science*, **298**(5599): 1737-1742
- Patera AT (1984) A spectral element method for fluid dynamics: Laminar flow in a channel expansion, *Journal of Computational Physics*, **54**(3): 468-488
- Shang S and Yun G J (2013) Stochastic finite element with material uncertainties: Implementation in a general purpose simulation program, *Finite Elements in Analysis and Design*, **64**(0): 65-78
- Witkowski W, Rucka M, Chró cielewski J and Wilde K (2012) On some properties of 2D spectral finite elements in problems of wave propagation, *Finite Elements in Analysis and Design*, **55**(0): 31-41
- Ziari S, Ezzati R and Abbasbandy S (2012) Numerical Solution of Linear Fuzzy Fredholm Integral Equations of the Second Kind Using Fuzzy Haar Wavelet, Advances in Computational Intelligence, S. Greco, B. Bouchon-Meunier, G. Coletti et al., Springer Berlin Heidelberg, **299**: 79-89

